Journal Homepage: - www.journalijar.com
INTERNATIONAL JOURNAL OF ADVANCED RESEARCH (IJAR)
Article DOI: 10.21474/IJAR01/1263
DOI URL: http://dx.doi.org/10.21474/IJAR01/1263
ISSN NO. 2320-5407

RESEARCH ARTICLE

Non-uniform Spectrum Sensing using Multicoset Sampling.

C. Raviteja and C. Subhas.
Sree Vidyaniketan Engineering College, Tirupati, India.

Manuscript Info

Manuscript History

Received: 15 June 2016
Final Accepted: 22 July 2016
Published: August 2016

Key words:-
Non-uniform sub-Nyquist sampling, Multicoset sampling, Cognitive radio, Spectrum sensing.

Abstract

Spectrum sensing is the core and key task of the Cognitive Radio. In this paper, we propose a spectrum sensing technique based on the estimates of the spectrum of a multiband signal obtained from its non-uniform multicoset sampler operating at the sub-Nyquist rate. We show that our proposed spectrum sensing method provides accurate results using fewer data samples. We discuss in detail the effect of false detections based on the signal reconstructed from non-uniform multicoset samples.

Introduction:-

The available electromagnetic radio spectrum is a precious resource, but it is not utilized efficiently because at a particular geographical location and time only a fraction of the entire spectrum is used. This effect combined with the current static licensing approach of the spectrum gives rise to unused spectrum white spaces or spectrum holes. Cognitive Radio (CR), a new way of looking at wireless communications, has the potential to become the solution to the spectrum underutilization problem, by permitting unlicensed users to utilize these spectrum holes [1]. The key task of CR is Spectrum sensing, defined as detecting the presence or absence of a signal by observing the radio spectrum. Some traditional spectrum sensing techniques are energy detection, matched filter and cyclostationary feature detection that have been proposed for narrow band sensing [2]. All these techniques filter the received signal with narrowband band-pass filters and then sample it uniformly at the Nyquist rate and then process the signal. In these approaches to spectrum sensing, the detection method is based on binary hypothesis-testing problem i.e. to detect the presence (H1) or absence (H0) of a primary user in the considered band.

With the advances in wireless communications, future cognitive radios should be capable of scanning a wideband of frequencies, over a few GHz. The usual sampling of a wideband signal needs high sampling rate ADCs, which are required to operate at or above the Nyquist rate. The spectrum sensing techniques mentioned above have their respective advantages and disadvantages. However, a common drawback is that they operate at Nyquist sampling rate. A major challenge is the development of efficient techniques to process the wideband signal sampled at Nyquist rate in real-time.

To overcome this problem, compressive sensing based solutions have been proposed in [3], [4] and [5]. In [3], authors proposed method based on Analog to Information converter. From the compressed samples of the signal, the spectrum can be estimated by solving an optimization problem. Wireless signals are typically sparse in the frequency domain. Using this fact in [5], a sensing method based on MUSIC algorithm has been proposed. It

Corresponding Author:- C. Raviteja
Address:- Sree Vidyaniketan Engineering College, Tirupati, India.

estimates the signal in time domain directly from its multicoset samples and spectrum holes are detected using subspace methods. Authors also showed that the proposed method would bring substantial saving in terms of the sampling rate at low spectrum occupancy. However, more data samples are required at low SNRs to detect the signal correctly.

In this paper, based on the sparsity of wideband signals in the frequency domain and using non-uniform sub-Nyquist Multicoset sampling of the input signal, we propose a wideband spectrum sensing method for the detection of active bands which reduces the average sampling rate. At low SNR values, the performance of the proposed method is examined with fewer data samples and is found to produce accurate results. The impact of the false detections of the proposed sensing method is analyzed using the reconstructed signal in time domain. The remainder of the paper is organized as follows. Section II details signal model and problem statement. Section III, provides an overview of multicoset sapling. The proposed non-uniform spectrum sensing method is presented in Section IV. Numerical results are presented in Section V followed by the empirical evaluation of threshold in Section VI. The impact of the proposed method on the multicoset sampler is discussed in Section VII followed by conclusion in Section VIII.

Signal Model and Problem Statement:-

Let $x(t)$ be a real valued, finite-energy, continuous-time signal and let $X(f) = \int_{-\infty}^{\infty} x(t)e^{-j2\pi ft}$ be its Fourier transform. We treat a multiband signal model $\mathcal{M}$ in which $x(t)$ is band limited to $\mathcal{B} = \left[\frac{-F_{Nyq}}{2}, \frac{F_{Nyq}}{2}\right]$.

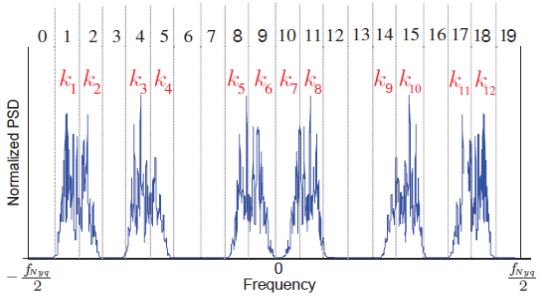

Fig.1:- Division of the observation band into L=20 cells where $K = \{\kappa_r\}_{r=1}^{12}$ are the indexes of the active cell.

$\mathcal{F}$ is the spectral support of the signal $x(t)$ such that $\mathcal{F} \subset \mathcal{B}$ and consists of at most N_B frequency intervals (bands) whose width is b.

Multicoset sampling starts by dividing the entire frequency band into L narrowband cells, each of them with bandwidth b, such that $F_{Nyq} = L \times b$ [6]- [7]. These cells are indexed from 0 to $L-1$, see Figure 1. Active cells are the spectral cells which contain part of the signal spectrum. The indexes of the active cells are collected into a set K called the active cells set where $K = \{\kappa_r\}_{r=1}^{q}$. Note that $q = |K|$, where $|*|$ is the cardinality operator. For the particular band shown in Figure 1, the set of active cells indexes is $K = \{\kappa_1, \kappa_2, \dots, \kappa_{12}\}$ = {1, 2, 4, 5, 8, 9, 10, 11, 14, 15, 17, 18} with q = 12 and NB = 6. To recover Nyquist rate samples of the received signal from sub-Nyquist Multicoset samples.

The knowledge of the number of bands N_B and K is of paramount importance [6] since they are required to reconstruct the time domain signal but are unknown to the system. Therefore, based on this discussion our problem is: *Given the observation band,* $\mathcal{B} = \left[\frac{-F_{Nyq}}{2}, \frac{F_{Nyq}}{2}\right]$, *the objective is to detect correctly the active cells set K for optimal reconstruction of the non-unifromly sub-nyquist sampled signal* $x(t)$ *and to analyze the impact of the false detection of K on the averaging sampling rate of the system.*

Multicoset Sampler:-

Figure 2 shows the complete block diagram of a Multicoset sampler and the proposed non-uniform spectrum sensing scheme. The multicoset sampler samples the incoming analog signal at a rate lower than the Nyquist sampling frequency. Using these samples the non-uniform sensing block performs spectrum detection and computes the parameters N_B and K, which required for reconstruction of the signal in the reconstruction block.

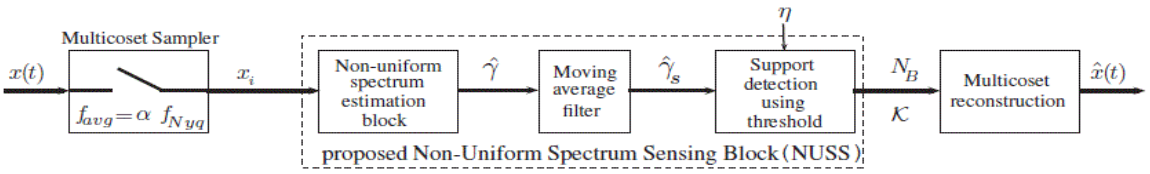

Fig. 2:- Multicoset sampler for Wideband signals along with the proposed Non-uniform Spectrum sensing method shown within the dotted block

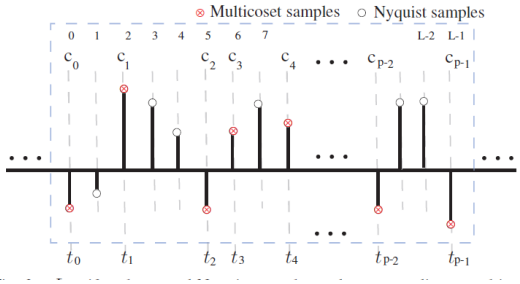

Fig. 3:- L uniformly spaced Nyquist samples and corresponding p multicoset samples.

In this paper, our objective is to study the performance of the proposed non-uniform sensing method. Therefore, we give an overview of the multicoset sampling scheme. Multicoset sampling is a periodic non-uniform sampling technique which samples the input signal $x(t)$ at a rate lower than the Nyquist rate, thereby capturing only the amount of information required for an accurate reconstruction of the signal based on the Landau lower bound [8].

Multicoset sampling starts by choosing an appropriate sampling period T, which is less than or equal to the Nyquist period of $x(t)$. Then the input signal $x(t)$ is non-uniformly sampled at $t_i(n) = (nL + c_i)T$, where $1 \leq i \leq p$ and $n \in \mathbb{Z}$ [9]. The sampling pattern is the set $\mathbb{C} = \{c_i\}$ which contains p distinct, unique integers from 0 to L-1 chosen to minimize the condition number [5]. The parameters L and p are selected such that $L \geq p > 0$.

Multicoset sampling can be viewed as first sampling the input signal at a uniform rate with period T and then selecting only p non-uniform samples from L uniform samples (see Figure 3). The process is repeated for consecutive segments each having L uniform samples such a way that the sampling period of the p selected samples is L.

The set $\mathbb{C}$ specifies the p samples such that $0 \leq c_1 \leq c_2 \leq \cdots \leq L-1$. Multicoset sampler can be implemented using p ADCs working in parallel [10]. Each ADC operates uniformly at a period $T_s = LT$. The multicoset sampler, provides p data sequences for i = 1… p, given by

$$x_i = x(nL + c_i)T = (n + \frac{c_i}{L})T_s \quad (1)$$

where $1 \leq i \leq p$. Therefore, the average sampling rate of the multicoset sampler is $F_{avg} = \alpha F_{Nyq}$, where $\alpha = \frac{p}{q}$. To recover the signal $x(t)$ sampled at the sub-Nyquist rate, N_B and K must be known to the reconstruction block [6].

Proposed Non-Uniform Spectrum Sensing Model:-

In this section, we discuss our proposed Non-Uniform Spectrum Sensing Block (NUSS) (shown in dotted block in Figure 2) to compute the parameters N_B and K which can allow successful reconstruction of $x(t)$. The function of each sub-block is explained in the subsections to follow,

Non-uniform spectrum estimation block:-

As stated in Section II, our objective is to detect the total number of bands N_B and the set of active cells K. Since the input signal $x(t)$ is under sampled and the samples are unevenly spaced, the usual spectrum sensing techniques like FFT based energy detection and cyclostationary based detection cannot be used [2]. To overcome this hurdle, we treat this scenario as a missing data problem and in this paper we propose to use the Lomb-Scargle method [11] to estimate the power spectral density (PSD) of the non-uniformly sampled signal. In the remaining sub-blocks of the sensing model, N_B and K are computed from this estimated PSD. The Lomb-Scargle periodogram is a popular tool

to detect if an unevenly spaced data is due to noise or it also contains the contribution of a signal by providing an estimate of the PSD.

Lomb-Scargle method [12] evaluates the samples, only at times t_n that are actually measured. Suppose that there are N_s samples $x(t_n)$, n = 1... Ns. The PSD estimate obtained from Lomb-Scargle method is defined by (1) (spectral power as a function of angular frequency $\omega = 2\pi f > 0$ with $f \subset B = [\frac{-f_{Nyq}}{2}, \frac{f_{Nyq}}{2}]$).

$$\hat{\gamma} = \hat{\gamma}(\omega) = \frac{1}{2\sigma^2}\frac{[\sum_i (x_i - \overline{x_i})\cos\omega(t_i - \delta)]^2}{\sum_i \cos^2\omega(t_i - \delta)} + \frac{1}{2\sigma^2}\frac{[\sum_i (x_i - \overline{x_i})\sin\omega(t_i - \delta)]^2}{\sum_i \sin^2\omega(t_i - \delta)} \quad (2)$$

Where $\overline{x}$ and σ^2 represent the mean and variance of the samples

Moving average filter block:-

It is observed that the PSD estimate $\hat{\gamma}$ obtained from the Lomb-Scargle method has a high variance. As a result of which N_B and K are not easy to detect if the PSD estimates are used in their original form. Therefore, we use a moving average filter to smoothen the $\hat{\gamma}$ obtained from the non- uniform sampled data. The moving average filter smoothes the incoming $\hat{\gamma}$ by replacing each data point with the average of the neighboring data points defined within a specified span.

This process is equivalent to low-pass filtering with the response of the smoothing given by the difference equation

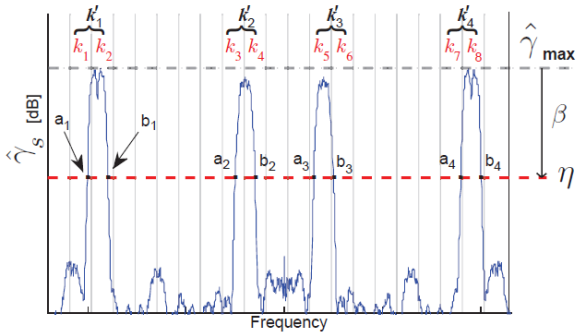

Fig. 4:- Support detection using threshold in non-uniform spectrum sensing block

$$\hat{\gamma}_s(f) = \frac{1}{2M+1}(\hat{\gamma}(f+M) + \hat{\gamma}(f+M-1) + \cdots + \hat{\gamma}(f-M)) \quad (3)$$

Where $\hat{\gamma}_s(f)$ is the smoothed value for the PSD at the frequency$f$, M is the number of neighboring data points on either side of $\hat{\gamma}_s(f)$ where 2M+1 is the span.

Support Detector Block:-

Once a smooth PSD estimate has been obtained, the spectral support F is computed with reference to a threshold value, η which is selected as a function of maximum PSD value $\hat{\gamma}_{max}$, i.e.,

$$\eta = \lfloor \hat{\gamma}_{max} + \beta \rfloor \quad (4)$$

where $\lfloor * \rfloor$ is the floor function. If $\hat{\gamma}_s$ is normalized such that $\hat{\gamma}_{max} = 0$ dB then $\eta = \beta$ dB, where β is negative valued. Selection of β plays a critical role in the performance of the proposed method. With reference to threshold η, the number of bands N_B are computed. The process is illustrated in Figure 4 for a signal with N_B=4. The spectral support is calculated using the following equation

$$F = \bigcup_{i=1}^{N_B} [a_i, b_i] \quad (5)$$

where a_i and b_i represent the crossing points at the threshold η. Once the support F is found, the set K can be calculated using (6) as follows

$$\lfloor a_i LT \rfloor \leq \{k_i\} \leq \lfloor b_i LT \rfloor \tag{6}$$

Where $1 \leq i \leq N_B$ and $T = \frac{1}{f_{nyq}}$.When all the k_i sets are calculated for each band, the set of spectral indexes K is computed as

$$K = \bigcup_{i=1}^{N_B} [\, k_i \,] = \{k_r\}_{r=1}^{q} \tag{7}$$

The set *K* then is sent to the reconstruction stage to recover $\hat{x}(t)$, as shown in Figure 2.

Performance of The Proposed Non-Uniform Detector:-

In this section, we present some numerical results for our proposed non-uniform spectrum sensing block. For simulations, the wideband of interest is in the range of $\mathcal{B}$ = [−300, 300] MHz, therefore, the Nyquist sampling rate is F_{Nyq} = 600 MHz we consider a multiband signal with N_B = 6 bands, each with a maximum bandwidth of *b*=10 MHz. Therefore, the input signal is sparse in the frequency domain. For simplicity we consider the N_B bands having the same amplitude. 16 QAM modulation scheme is used to transmitted the signal that is corrupted by the additive white Gaussian noise channel.

Given F_{max} = 300 MHz, it is desired to detect N_B and *K* for the input signal which is sampled at a sub-Nyquist rate using the multicoset sampler. For the NUSS block β is set equal to -3.5 dB. The performance of the proposed system is evaluated by computing the probability of correctly detecting the occupancy of signal and probability of false alarm in terms of N_B and *K* as follows

$$P_{d(N_B)} = \Pr\left(\widehat{N_B} = N_B\right)$$
$$P_{d(K)} = \Pr\left(\widehat{K} = K\right) \tag{8}$$

$$P_{fa(N_B)} = \Pr\left(\widehat{N_B} > N_B\right)$$
$$P_{fa(K)} = \Pr\left(\left|\widehat{K}\right| > |K| \middle| \left|\widehat{K}\right| \subset |K|\right) \tag{9}$$

Equation 9 gives the probability of false alarm (P_{fa}) where $|K|$ represents the cardinality of *K*. The subscripts N_B and *K* are used to distinguish the probabilities for the number of bands and the active cell set, respectively. We present both the $P_{d(K)}$ and $P_{d(N_B)}$ as the correct detection probability of the active cells and the probability of correct detection of N_B, see equations (8) and (9). We have performed 1000 iterations at various values of α to compute P_d and P_{fa}. Results in Figures (5-8) are plotted explicitly to show the performance of the NUSS block. Furthermore the results are compared with the energy detector. The results for energy detector are plotted for P_{fa}=0.01 [13].

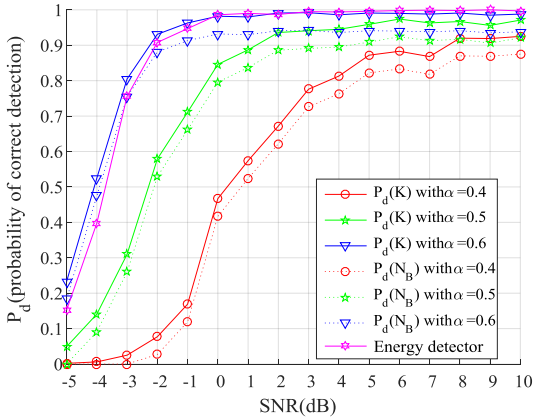

Fig. 5:- $\boldsymbol{P_{d(K)}}$ and $\boldsymbol{P_{d(N_B)}}$ plotted against varying SNR for $\boldsymbol{\alpha}$= 0.4, 0.5, 0.6.

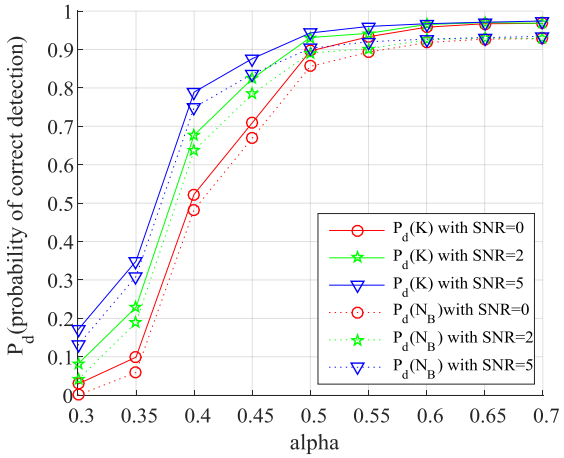

Fig. 6:- $\boldsymbol{P_{d(K)}}$ and $\boldsymbol{P_{d(N_B)}}$ plotted against varying $\boldsymbol{\alpha}$ for different SNR

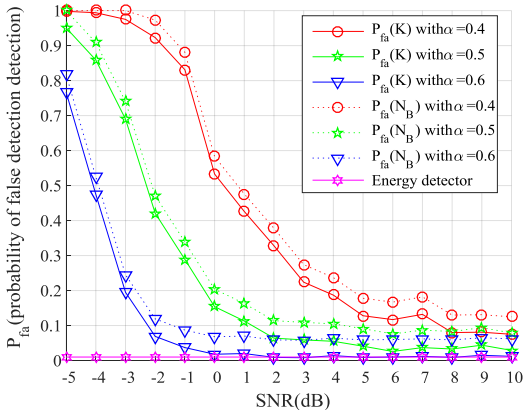

Fig. 7:- $\boldsymbol{P_{fa(K)}}$ and $\boldsymbol{P_{fa(N_B)}}$ plotted against varying SNR for $\boldsymbol{\alpha}$= 0.4, 0.5, 0.6.

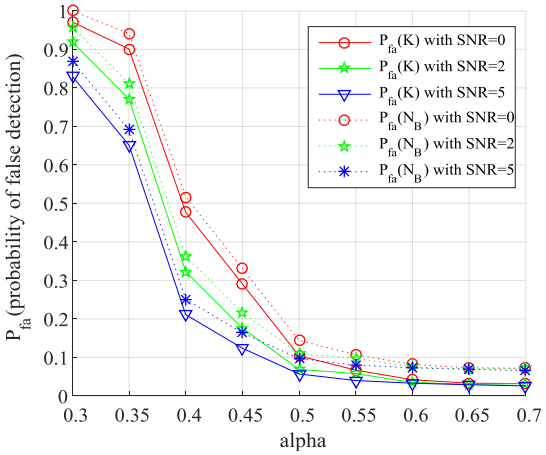

Fig. 8:- $P_{fa(K)}$ and $P_{fa(N_B)}$ plotted for varying α at different SNR

In Figure 5, $P_{d(K)}$ and $P_{d(N_B)}$ are plotted against varying SNR for α= 0.4, 0.5, 0.6. It is observed that for α= 0.4, at low SNR, i.e., below 0 dB $P_{d(K)}$ is low and $P_{d(K)}$ increases as SNR is increased reaching close to 1.

At α= 0.5, the performance is better after SNR= 2dB. With α= 0.6, even better performance is obtained, and the results are close to the energy detector. The common pattern observed here is that as SNR increases P_d increases and saturates at a particular SNR value because of less noise and both $P_{d(k)}$and $P_{d(N_B)}$ are close and follow the pattern mentioned above.

In Figure 6 where $P_{d(K)}$ and $P_{d(N_B)}$ are plotted for various values of α. The proposed sensing model behaves poorly at α=0.3, but its performance improves at α=0.4. At α=0.5, our proposed sensing model detects with high probability, and it gets close to 1 for α=0.7. Figure 6 shows that the performance of the proposed sensing method depends on the number of non-uniform samples available at the NUSS block for detection.

In figure 7, we plot $P_{fa(N_B)}$ and $P_{fa(K)}$ as a function of varying SNR. At low SNR, i.e., at -5dB the values of $P_{fa(N_B)}$ and $P_{fa(K)}$ are high. Bur as SNR increases, $P_{fa(N_B)}$ and $P_{fa(K)}$ drop quickly, becoming close to zero at SNR=1 dB. At α= 0.6, the performance of proposed method matches the performance of the energy detector for SNR above 1dB. $P_{fa(N_B)}$ and $P_{fa(K)}$ also depends on the number of non-uniform samples available. This can be explained using Figure 8, where $P_{fa(N_B)}$ and $P_{fa(K)}$ are plotted for various values for α**.** As α increases from 0.3 to 0.7, P_{fa} drops rapidly reaching close to zero due to the availability of more number of samples. It is observed that performance of the sensing model improves with increasing α**.**

Empirical Evaluation of β:-

As seen from the previous section, the threshold η depends on β. This section provides the empirical evaluation of β. Optimum values of β result in a higher difference between P_d and P_{fa} given in equation (10). For simplicity of explanation, in this section, we only present results for detection of spectral indexes *K*.

$$\Delta P = P_d - P_{fa} \qquad (10)$$

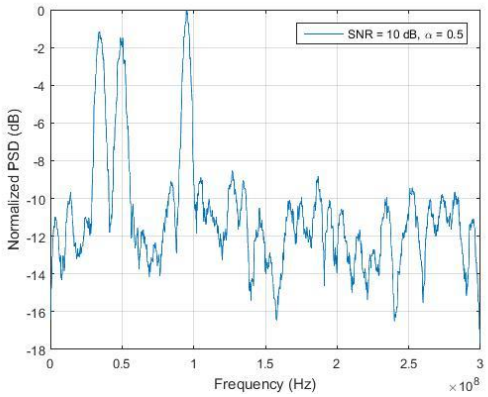

Fig. 9:- Normalized PSD estimate obtained from NUSS block

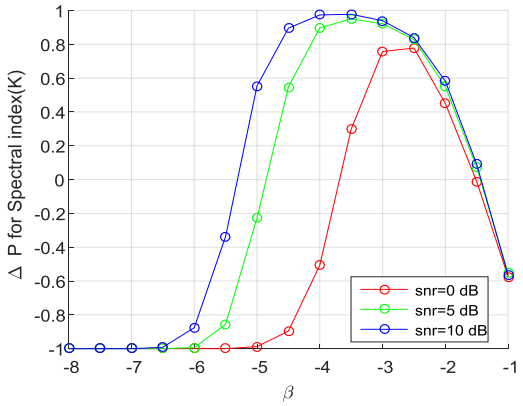

(a) α = 0.4

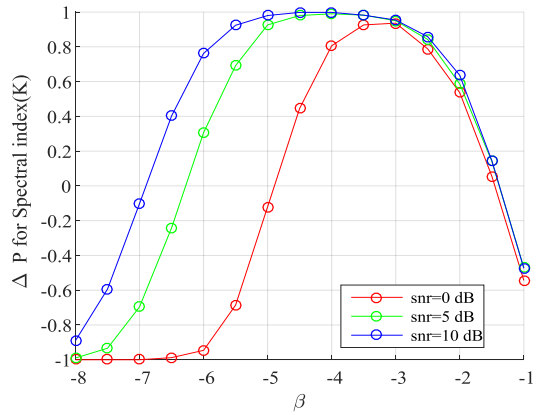

(b) α = 0.5

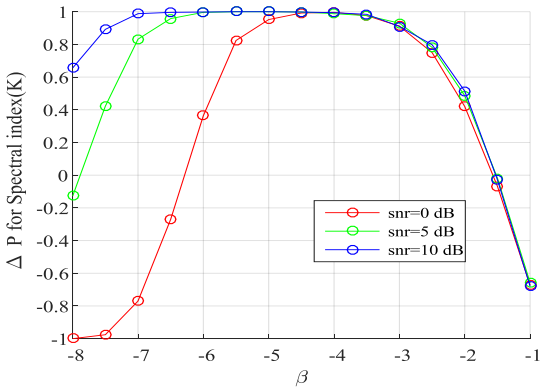

(c) α = 0.7

Fig. 10:- Selection of optimal value of threshold η.

Also, the PSD estimate obtained from the moving average filter of the NUSS block is normalized such that $\hat{\gamma}_{max}$ =0 dB and therefore from equation (4), $\eta = \beta$.The signal parameters are the same as were in Section V. 1000 Monte-Carlo iterations are performed to find β empirically β.

Figure 9 shows the PSD estimate for α=0.4 and SNR=10dB. In figure 10, we have plotted ΔP against varying β values for α=0.4, 0.5 and 0.7 for three values of SNR, i.e., 0, 5, 10 dB. From Figure 10(a), we observe that for small α=0.4, maximum values of ΔP occur between β = -4.5 dB and β = -3 dB but ΔP does not reach one because of the small number of samples available.

In Figure 10(b), α=0.5, ΔP is higher compared to α=0.4 in Figure 10(a) also maximum ΔP is observed between β = -5.5 dB and β = -3 dB because of availability of more number of samples. In Figure 10(c), α=0.7 ΔP reaches even at low SNR due to the availability of more number of samples. Maximum ΔP is observed between β = -6 dB and β = -3 dB at the cost of more number of samples also the reconstruction is less noisy.

From the results in Figure 10, it is observed that β= -3.5 dB is within the optimal ΔP range for the three values of α and SNR considered which can be selected to establish a trade-off between α and detection performance.Therefore, in this paper, we have selected β = -3.5 dB which provides satisfactory results as was shown in the numerical results in Section V.

Reconstruction Performance:-

In this section, we analyze the impact of false detections of the proposed non-uniform sensing method on the reconstruction of $x(t)$ shown in Figure 2. The performance is analyzed in terms of the RMSE (Root Mean Squared Error) of the reconstructed time domain signal, i.e,

$$RMSE = \frac{\|\hat{x}(t) - x(t)\|_2}{\|x(t)\|_2} \quad (11)$$

The simulation parameters are the same as were in Section V, i.e., A multiband signal with $\mathcal{B}$ = [-300 MHz, 300 MHz] and the Nyquist sampling rate is f_{max} =600 MHz and N_B=6.

In Figure 11, RMSE is plotted against SNR values for α=0.3 and 0.4 for non-blind multicoset sampler and blind multicoset sampler. The non-blind multicoset sampler has perfect knowledge about the number of bands N_B and spectral indexes *K* of the input signal while blind multicoset sampler uses the proposed NUSS block to estimate N_B and *K*. It is observed that for α = 0.3, the RMSE for blind multicoset sampler is very high compared to RMSE for the non-blind multicoset sampler. This is because of the high number of false detections provided by the NUSS block at α = 0.3. However for α = 0.4, the performance of the NUSS block improves for SNR values greater than 5 dB, and it is observed that the RMSE for blind multicoset sampler matches that of the non-blind multicoset sampler.

To summarize the performance of the proposed sensing method we have plotted RMSE against varying values of α for different SNR values in Figure 12. We can observe from RMSE curves that the performance of the proposed non-uniform sensing method is poor at α = 0.3 even at high SNR because of highP_{fa}. Furthermore, as α increases RMSE reduces because more number of samples are available for reconstruction and P_d is high.

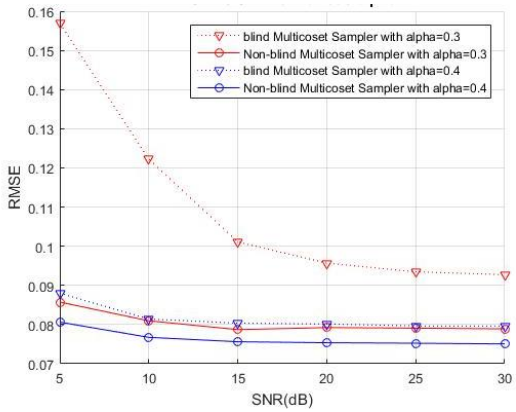

Fig. 11:- Comparison of blind and non-blind multicoset samplers in terms of RMSE plotted against various SNR values

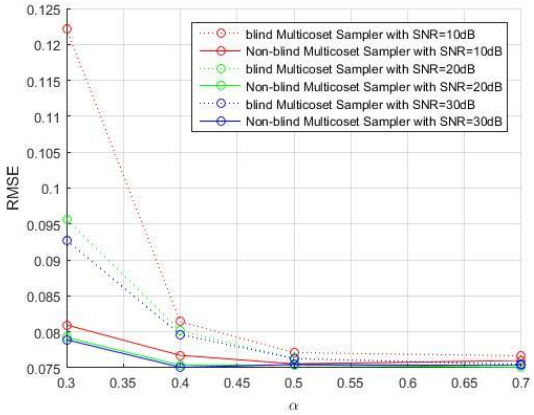

Fig. 12:- Comparison of the non-blind and blind multicoset sampler in terms of RMSE plotted against various values of α

Conclusion:-

In this paper, we have proposed a spectrum sensing technique based on non-uniform sub-Nyquist multicoset sampling. We have shown that the proposed sensing method shows high detection and low false alarm probabilities also the performance of the proposed method improves with the increase in the number of the non-uniform samples. Finally, the effect of false detection is shown using RMSE of the reconstructed time domain signal.

References:-

1. S. Haykin, "Cognitive Radio: Brain-empowered wireless communications," *IEEE Journal on Selected Areas in Commincations*, vol. 23, no. 2, pp. 201-220, Feb 2005.
2. Y. C. Lang, A. T. Hoang and R. Zhang Y. Zeng, "A review on Spectrum Sensing for Cognitive radio: challenges and solutions," *EURASIP J. Adv. Signal process*, vol. 2010, pp. 2:2-2:2, Jan 2010.
3. Y. Wang, A. Pandharipande and G. Leus Y. Polo, "Compressive wideband spectrum sensing," *IEEE International Conference on Acoustics, Speech and Signal Processing (ICASSP)*, pp. 2337-2340, April 2009.
4. Z.Tian and G. Giannakis, "Compressed sensing for wideband cognitive radios," *IEEE ICASSP*, vol. 4, pp. IV-1357-IV-1360, April 2007.
5. K. Haghighi, A. Owrang and M. Viberg M. Rashidi, "A wideband spectrum sensing method for cognitive radio using sub-nyquist sampling," *Digital SignalProcessing Workshop and IEEE Signal Processing Education Workshop (DSP/SPE)*, pp. 30-35, Jan 2011.
6. M. Rashidi, "Non- uniform sampling and reconstruction of multiband signals and its application in wideband spectrum sensing of cognitive radio," *CoRR*, vol. abs/1010.2518, 2010.
7. M. Rashidi and Y. C. Eldar, "Blind multiband signal reconstruction: Compressed sensing for analog signals," *IEEE Transactions on Signal Processing*, vol. 57, no. 3, pp. 993-1009, Mar 2003.
8. R. Venkataramani and Y. Bresler, "Optimal sub-nyquist sampling and reconstruction of multiband signals," *IEEE Transactions on Signal Processing*, vol. 49, no. 10, pp. 2301-2313, 2001.
9. M. Mishali and Y. C. Eldar, "From theroy to practice: Sub-nyquist sampling of sparse wideband analog signals," *IEEE Journal of Selected Topics in Signal Processing*, vol. 4, no. 2, pp. 375-391, 2010.
10. B. Aziz and D. Le Guennec S. Traore, "Dynamic single branch non-uniform smapler," *International Conference on Digital Signal Processing (DSP 2013)*, Feb 2013.
11. J. D. Scargle, "Studies in astronimical time series analysis II. statistical aspects of spectral analysis of unevely sampled data," *Astrophysical Journal*, vol. 263, pp. 835-853, 1982.
12. Samba Traor´e, Amor Nafkha and Daniel Le Guennec Babar Aziz, "Spectrum Sensing for Cognitive Radio," *IEEE Global Communications Conference*, pp. 816-821, Dec 2014.
13. K. Haghighi, A. Panahi nad M. Viberg M. Rashidi, "A nlls based sub-nyquist rate sectrum sensing for the wideband cognitive radio," *IEEE Symposium on New Frontiers in Dynamic Spectrum Access Networks (DySPAN)*, pp. 545-551, May 2011.